GOLD 2006 PRESENTATION

Preparation of Nanoscale Gold Structures by Nanolithography

Nicholas Stokes, Andrew M McDonagh,* Michael B Cortie

* Institute for Nanoscale Technology
University of Technology, Sydney
PO Box 123 Broadway NSW 2007 Australia
Telephone: +61 2 9514 1035
Fax: +61 2 9514 1703
Email: andrew.mcdonagh@uts.edu.au

Abstract

Gold is the material of first choice for the realisation of a large number of interesting nanoscale devices and structures due to its unique chemical and optical properties. However, conventional photolithographic processes cannot be used to manufacture such tiny structures in gold (or any other material) due to limitations imposed by the diffraction of light. New methods of lithography have been developed to overcome this limitation. In this article we review these new nanolithographic techniques, describe how they have been used to produce nanoscale precious metal artefacts, and briefly survey some of the existing and potential applications for these structures.

1 Introduction

The rapid and highly successful development of optical lithography has powered society's extraordinary development of information technology. In conventional optical lithography, light is directed through a finely detailed mask onto a layer of photoresist that lies on the surface of a silicon wafer. The resulting patterns of illumination are used to selectively alter specific regions on the photoresist, which after several iterations of chemical treatment become the transistors, tracks and other features of modern integrated circuits. Unfortunately, diffraction of light with wavelength, , normally limits the resolution that can be achieved to about l/2, which translates to a few hundreds of nanometers if visible light is used.

However, there are a great many reasons why fabrication of metallic patterns with finer feature sizes would be useful. Of course, most metals oxidise readily under ambient conditions, and the thickness of the resulting oxide layer may vary from tens to millions of nanometers. Such oxide layers are sufficiently thick in many cases to completely negate the desired functionality of the nanoscale structure. This is one of the reasons why gold, which does not form an oxide layer under ambient conditions, is so extensively used in nanoscale technology. Gold is also readily and conveniently deposited by commonly available techniques such as electroplating, electroless deposition and thermal evaporation. Gold not only also has useful optical characteristics that commend its use in many applications operating in the visible and infrared region of the spectrum, but it additionally has a controllable thiophilic surface chemistry (affinity for thiol or sulfhydryl (SH) groups). This property allows complex and useful layers of organic molecules to be assembled on gold surfaces. It is for these various reasons that gold is so attractive for use in diverse nanotechnological investigations.[1]

Naturally, the issue of how to fabricate gold structures at resolutions significantly finer than those routinely used in optical lithography arises. We will show here that this topic has attracted extensive interest and investigation, and in this paper we provide a succinct and up-to-date review of the field. We focus on the techniques by which nanoscale gold shapes such as spheres, circles, rods, lines, rings, cylinders, crosses, and squares [2-14] have been produced, ignoring the more voluminous literature on semiconductor lithography. We conclude by providing a brief description of some of the nanoscale gold devices and optical applications that require sub-wavelength lithography for their realisation.

2 Nanolithographic methods

Lithography is a method for printing onto surfaces and has been used for centuries. Nanolithography refers to the fabrication of structures where at least one lateral dimension lies in the range of 1 to 100 nm. There have been several good reviews focusing on some of the standard

nanolithographic techniques [15-18] and the reader is referred there for generic background information. We present here information to enable the reader to appreciate the applicability of each technique to fabricating precious metal nanostructures.

2.1 Electron beam lithography

Electron beam lithography (EBL) uses an electron beam focused onto a substrate coated with a beam-sensitive material and the beam is directed to produce a specific pattern. Because the diffraction limit of electrons is much smaller than that of visible, UV or even X-ray photons, the spatial resolution of EBL is greater than techniques using these beam sources. EBL can be used to create nanostructures directly or to construct masks for use with other lithographic techniques.

Gotschy *et al.* used EBL to create metal dot arrays on transparent glass substrates.[19] We draw attention to the fact that insulating substrates complicate the EBL process due to charging effects. This occurs when electrons cannot dissipate from the surface quickly enough, and regions of the sample where the beam strikes become negatively charged and cause incoming beam electrons to be repelled. Often this results in images drifting and a skewing of patterns. To prevent charging, the nonconductive substrate requires a conductive layer to disperse excess electrons. Antimony-doped tin oxide,[11] indium-doped tin oxide (ITO) [14, 19-22] and fluorine tin oxide (FTO) all form reasonably transparent conducting layers that will allow EBL to be performed on glass substrates. Gotschy *et al.* used a thin layer of ITO applied by sputtering. A 60 nm polymethylmethacrylate (PMMA) e-beam resist was spin-coated onto ITO-coated glass and an electron beam used to expose a dot array pattern. The exposed resist was removed with solvent and a 10 - 50 nm silver metal layer was then deposited by thermal evaporation. The remaining PMMA layer, together with the excess silver deposited on it, was removed by acetone leaving the silver dot array on the ITO glass.[19]

Lamprecht *et al.* utilized the same procedure except that circular gold nanostructures in two-dimensional arrays were fabricated.[20] EBL allowed the particle shape and interparticle distance in the arrays to be varied independently. The optical effects of plasmon excitation were investigated (see Section 3.2.).

Ueno *et al.* also used a similar process to create arrays of gold rods.[2] A 2 nm Cr / 60 nm Au bilayer was deposited onto a mask prepared by EBL; the chromium reportedly improves binding of the gold to the substrate. Arrays of gold rods with aspect ratios (aspect ratio is the ratio of length to width) varying between 1 and 9 were prepared. Figure 1 shows an array of rods with aspect ratio of 9.

Metamaterials are materials that gain their electromagnetic properties from structure rather than the material it is composed from. Metamaterials composed of split ring resonators (SRRs) have been fabricated using EBL by several groups.[21-23] The split rings consist of gold 20 - 30 nm thick and with variable lateral dimensions. The resonators were fabricated in a 100 μm^2 periodic array using PMMA resist on an ITO glass substrate. The pattern and dimensions are shown in Figure 2. Optical properties of SRRs have been investigated, and allow the possibilities of negative permittivity and negative permeability at specific wavelengths depending on the resonant frequency of the circuits' structures. Both negative permittivity and permeability give rise to negative refractive index materials. This implies that electrons within the sample move in the opposite direction of the applied electric and magnetic fields.[24, 25] Other metamaterials have been fabricated from different shaped structures. Grigorenko *et al.* used EBL to fabricate gold pillars (flat topped cones) 80-90 nm high and ~ 100 nm diameter on a glass

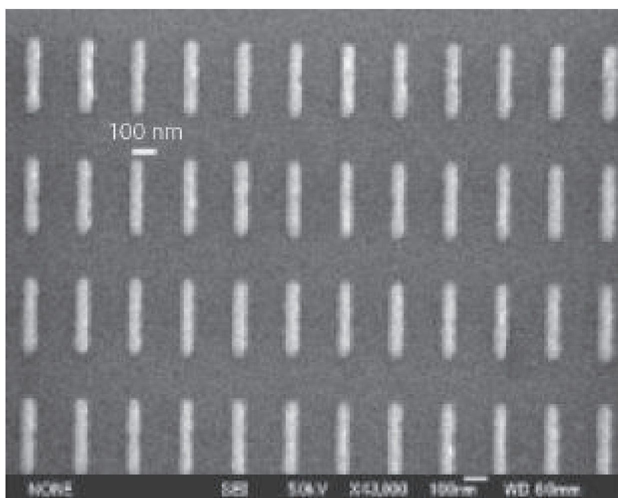

Figure 1
Array of gold nanorods with aspect ratio of 9. Each rod has dimensions of 40 nm (w) x 360 nm (l) x 60 nm (h) and spaced 200 nm apart. Reprinted with permission from Ref. 2, Ueno et al., Opt.Lett., ***30****, 2158 (2005). © 2005 Optical Society of America*

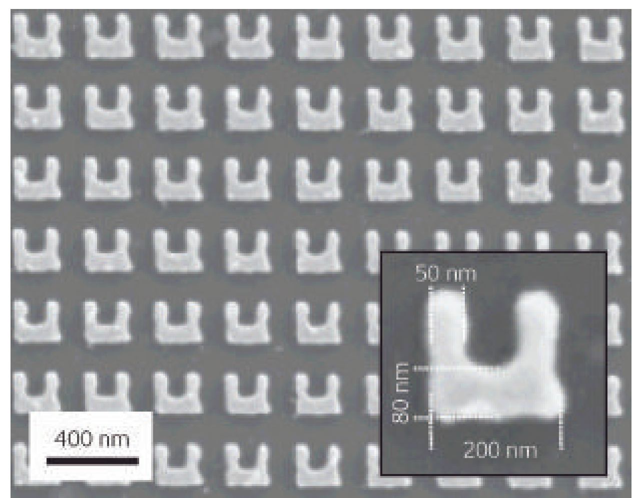

Figure 2
SEM image of a 100 μm^2 array of SPRs. The insert shows the dimensions of an individual split ring. Reprinted with permission from Ref. 22, Enkrich et al., Phys. Rev. Lett., ***95****, 203901 (2005). © 2005 The American Physical Society*

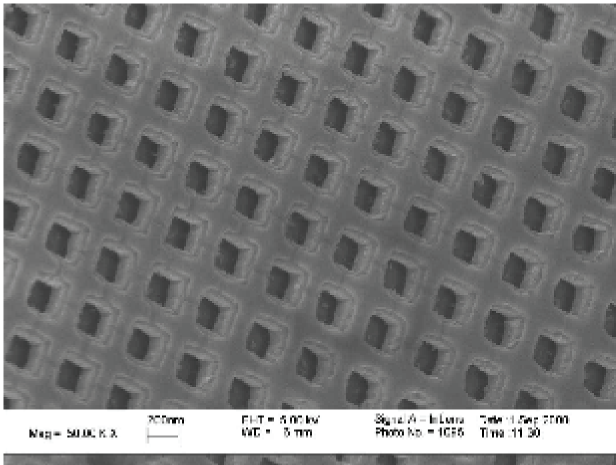

Figure 3
*Gold grid to filter infrared radiation. Reprinted from Ref. 8, Jefimovs et al., J. Mod. Opt., **51**, 1651 (2004) by permission of Taylor & Francis Group. © 2004 Taylor & Francis Ltd (http://www.tandf.co.uk/journals)*

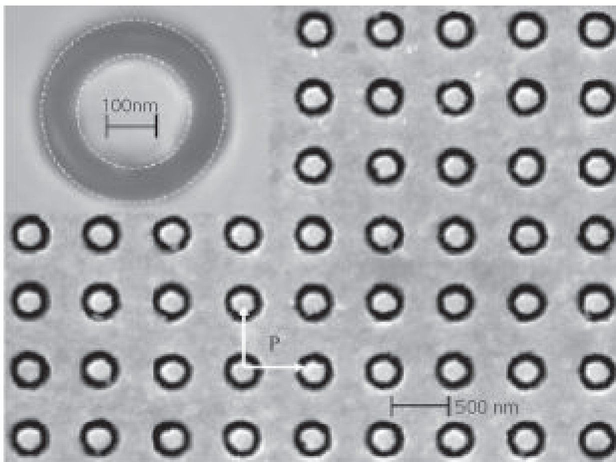

Figure 4
*SEM image of the annular aperture array pattern after lift-off. Ring diameter 225/360nm (ID/OD). Reprinted with permission from Ref. 11, Perentes et al., Nanotechnology, **16**, S273 (2005). © 2005 IOP Publishing Ltd*

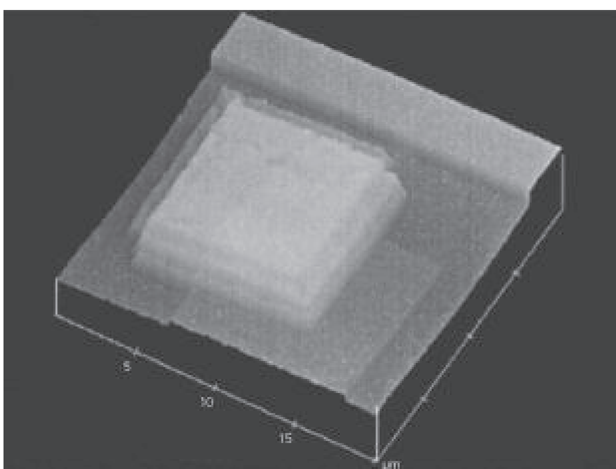

Figure 5
AFM image of a four-layered test structure. Reprinted with permission from Ref. 28, Griffith et al., J. Vac. Sci. Technol. B, **20**, *2768 (2002). © 2002 American Vacuum Society*

substrate and grouped in tightly spaced pairs.[26] Garwe *et al*. have also used EBL and ion beam lithography to create a potential metamaterial.[27] Gold wires 200 x 500 nm with thickness 75 nm were fabricated on glass as a single layer, a double layer with 180 nm PMMA spacer and a double layer with 600 nm layer spacer.

Jefimovs *et al*. created nanostructures to filter infrared radiation.[8] On a conducting gold substrate, a thick (300 - 800 nm) layer of polyimide was applied by spin coating, followed by vapour deposition of a ~50 nm layer of SiO_2, spin coating of a ~100 nm layer of PMMA resist and, finally, sputtering of a ~20 nm conductive Al film to prevent charging during EBL.[8] A grid pattern was exposed using EBL through the Al layer into the PMMA resist. The thin PMMA layer has a very small interaction volume with the e-beam and enables small, well-defined structures to be formed. The PMMA was then developed with solvent to form a mask for a subsequent reactive-ion etching (RIE) step. The grid pattern was etched into the sublayers using RIE and gold was deposited by electroplating into the voids. Figure 3 shows the gold grid structure prepared.

Arrays of annular apertures in gold layers have been fabricated on antimony-doped tin oxide coated glass substrates (Figure 4).[11] In this procedure, a negative tone resist is used whereby sections not exposed to the e-beam are initially removed. A gold film was then deposited over the entire surface and when the remaining resist was removed, voids in the gold film, in the form of 100 nm rings, were revealed.

Griffith *et al*. developed an additive-layer technique for multiple-material functionality.[28] The procedure involves spin-coating a resist consisting of thiol-capped Au or Ag nanoparticles onto a silicon wafer, glass slide or polyimide film substrate. Exposure of the resist to an e-beam removes the stabilising thiol molecules, which results in aggregation of the metal nanoparticles. The unexposed resist was removed using solvent and the remaining sample was annealed to strongly bind the metal nanoparticles to the substrate. Successive layers can be spin-coated directly over previous structures.[28] Figure 5 shows a four layered structure with conformal layering, but includes some misalignment.

Fukushima *et al*. fabricated periodic gold nanostructures consisting of arrays of lines and dots using a somewhat different approach.[12] A sol-gel process was used to prepare SiO_2/TiO_2 containing chloroauric acid ($HAuCl_4$) and laser dyes, and the mixture was spin-coated onto a glass substrate. Gold nanoparticles were generated by reduction of the Au(III) ions using electron beam irradiation directed to form the desired shapes.

2.2 Nanolithography using beams of ions or atoms

A rather different type of nanolithography is possible if the beam is comprised of ions or atoms instead of electrons. There are three main ion-beam lithography (IBL) techniques, focused ion beam (FIB), proton beam writing (*p*-beam writing) and ion projection lithography (IPL).[29]

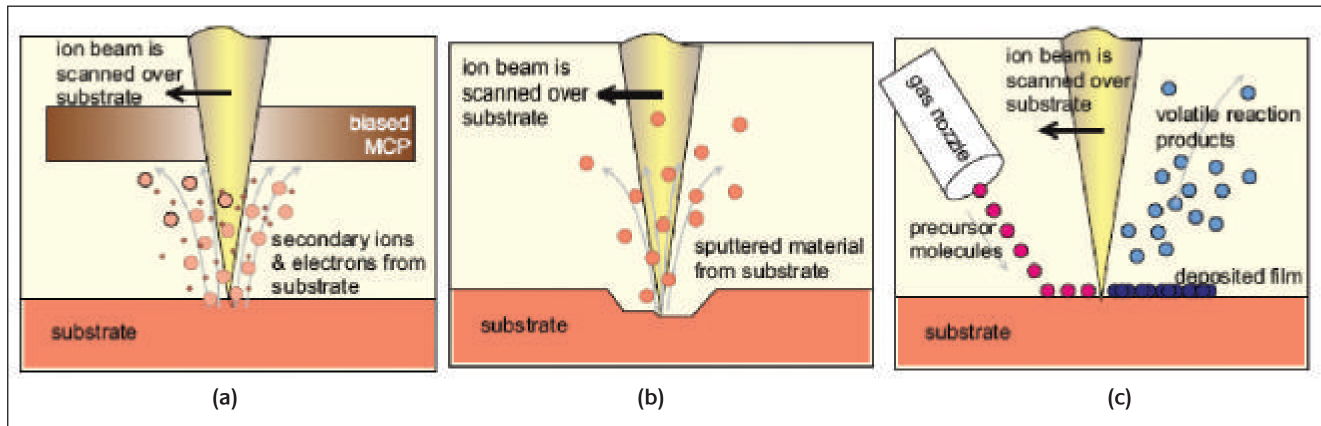

Figure 6

Principles of Focused Ion Beam, (a) imaging, (b) milling and (c) deposition. Reprinted with permission from Ref. 30, Reyntjens et al., J. Micromech. Microeng., ***11****, 287 (2001). © 2001 IOP Publishing Ltd*

Focused ion beam (FIB) involves a focused heavy-ion beam rastered over a surface creating a pattern through modification of the surface structure (either physically or chemically), deposition of atoms, or removal of atoms from the surface through sputtering.[29, 30] Ga or Ar ions are generally used. The processes involved in FIB are shown in Figure 6. The small penetration depth of heavy ions into the substrate allows complex 3-dimensional structures to be fabricated with high resolution.[29, 31-33] Patterns can be written into virtually any material, however the process is relatively slow.[29, 30, 34, 35] Etching rates may be increased by using reactive gasses,[29-35] or writing into materials like PMMA.[29, 36]

Hanarp *et al.* used focused ion-beam lithography to create arrays of gold disks.[13] A 20 nm thick gold film was deposited on a glass substrate and polystyrene nanoparticles were self-assembled onto the gold layer from a colloidal solution. The polystyrene particles act as a mask and an argon ion beam was used to etch the gold not covered by particles. The particles were then removed to leave gold disks. The size of the gold disks is controlled by the size of the masking polystyrene particles. Interestingly, the size of the polystyrene particles is temperature dependent, so changing the temperature alters the size of gold disks. This nanolithographic method is capable of producing optical coatings over large areas with controllable size, shape and interparticle spacing.[13]

Proton beam writing and ion projection lithography are related IBL techniques although no reports of precious metal structures have been forthcoming to date. Proton beam (*p*-beam) writing uses fast (MeV) protons to write deep, precise 3-dimensional patterns into resist layers.[29] The protons penetrate deep into the resist material with minimal surface disruption and little to no beam deviation aside from some end of range broadening. This aspect of *p*-beam writing is a significant advantage over EBL techniques in which the lighter electrons scatter far more readily, increasing the difficulty in maintaining very small line widths. Also, secondary electrons produced by the primary proton beam have low energy and therefore limited range, resulting in minimal proximity effects.[29, 37] *p*-Beam writing is effective in fabricating high aspect ratio and multi-layer structures within PMMA resist of gratings, columns and other 3D structures.[37]

Ion projection lithography (IPL) uses medium energy ions (~100 keV) projected through a patterned mask for fabrication. A beam of ions uniformly illuminates a large area patterned mask and the transmitted beam is projected onto the surface using electrostatic lenses. IPL has been used to pattern at 50 - 75 nm resolution using a single exposure.[29] With IPL there are no diffraction effects, and the depth of ion penetration is adjustable. The ability to pattern a large area in a single exposure without wet-chemical processing is also quite attractive.[29]

Atom lithography uses atomic beams to create structures on surfaces. There are two variants of the atom lithography process. One method uses a beam of reactive atoms to chemically modify a suitable resist, similar to the etching processes used in EBL and FIB. In the second method, the nanostructure is formed from atoms deposited directly by the beam in selected patterns. Mützel *et al.* utilized atom lithography with an optical light mask.[7] Optical dipole forces concentrated atoms near the nodes of a standing light-wave field. A holographic mirror was used to control a cesium atom beam to deposit a pattern onto a substrate consisting of silicon wafer covered with a 30 nm gold film and self-assembled monolayer of 1-nonanethiol. The 1-nonanethiol layer protects the gold during a wet chemical etching process. The deposited cesium structure attaches to the 1-nonanethiol layer, removing the protective action of the 1-nonanethiol to the etching process. Therefore the pattern defined by the cesium atoms is transferred into the gold layer.[7, 38]

2.3 Nanolithography using visible or ultra-violet light

Optical lithography is capable of producing sub-100 nm patterns with the use of very short wavelengths. Fabrication of sub-50 nm patterns requires the use of a liquid immersion technique and photomask enhancement technologies such

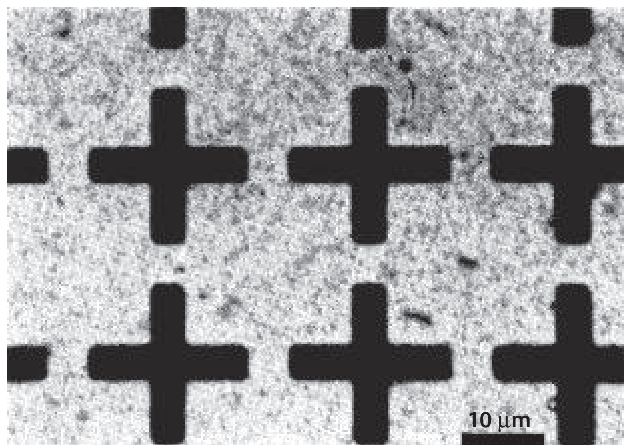

Figure 7

Micrograph of a gold resonant mesh on a 3 micron polyimide foil. Reprinted from Ref. 10, Johannsmann et al., Infrared Phys., **26**, *215 (1986) with permission from Elsevier*

as phase-shift masks and optical proximity correction. There have been several published reviews describing this area. [39-43]

Guo *et al*. used interference lithography to create gold gratings that can be used for optical applications.[44] A laser exposed a pattern in a sample consisting of 100 nm thick photoresist deposited onto a 40 nm thick gold film. The exposed resist was removed and the sample was etched using an ion beam to form the pattern in the gold layer. The remaining resist was removed to give the gold structures. Gold nanowire structures with line widths ranging between 115 nm to 200 nm were prepared. The process provides an inexpensive, fast, and versatile means for the fabrication of large area metallic nanostructures.[44]

Nakata *et al*. used lithographical laser ablation to fabricate gratings of lines and circular holes.[45] Light from a femtosecond pulsed laser was passed through a mask and the pattern was imaged onto a gold film on a silica-glass substrate by a coherent optical system. Periodic structures such as nano-sized hole matrices and nano-meshes were generated in a single shot of laser ablation.[45] This process created large area patterns rapidly but the resolution was lower than that using many other lithographic techniques.

Ultraviolet lithography is similar to optical lithography but uses shorter wavelength light resulting in a lower diffraction limit. Using appropriate mirrors and photomasks, the highest resolution reached to date has been slightly better than 30 nm through the use of interference lithography in the extreme ultra-violet region.[46, 47] This linewidth was achieved through Extreme Ultra-Violet Interference Lithography (EUV-IL) whereby extreme UV light is passed through two diffraction gratings simultaneously and the corresponding beams periodic interference pattern is exposed into a EUV resist.

Johannsmann *et al*. used UV lithography to create infra-red filters using a cross-shaped pattern in a gold layer (see Figure 7).[10] The structure was fabricated using a mask formed by EBL and then applying UV light through the mask onto a resist layer. The imaging accuracy is limited by the wavelength of the UV radiation and by the diffusion processes during the development of the photomaterial.

Recently, Sun *et al*. reported a procedure [48] similar to the EBL technique reported by Griffith *et al*.[28] Exposure of a film of thiol-stabilised gold nanoparticles on silicon by UV radiation oxidised the thiol molecules. The gold nanoparticles aggregated and formed structures that solvent did not remove. Using UV light to oxidise the thiol molecules allowed a mask to be used, giving micrometre-scale structures. The minimum line width produced was 60 nm for Langmuir-Schaeffer films using a UV laser attached to a near-field scanning optical microscope in place of a lamp and mask setup. The lamp and mask setup produced structures that were porous, whereas the UV laser produced dense, continuous structures.

Another recently developed optical lithography technique is zone-plate-array lithography (ZPAL).[49-51] ZPAL is a maskless optical technology that employs an array of optical lenses that focus incident light onto the substrate. A UV laser is reflected off a spatial-light modulator that directs light with adjustable intensity to individual zone plates, where the incident light is focused onto a resist. The zone-plate-array is fabricated using EBL. The substrate is scanned beneath the array and various patterns can be built up in a dot-matrix fashion.[49, 51] Minimum linewidths reported to date are ~ 115 nm.[49]

Envanescent Near-Field Optical Lithography (ENFOL) overcomes the diffraction limit of $\lambda/2$ by utilising the near-field's high-spatial frequency information and has been used to achieve $\lambda/7$ resolution.[52] ENFOL consists of a glass support with an attached tungsten mask produced by EBL which is brought into vacuum contact with a silicon substrate with a layer of bottom anti-reflection coating and a photoresist.[52-54] A UV light is shone through the mask and the pattern is transferred to the resist. This system requires contact between mask and resist which limits applications. Planar Lens Lithography (PLL) is a subset of ENFOL in which a planar silver lens is added into the system and illuminated near its UV electromagnetic-resonance which projects the near-field (super-lensing), removing the requirement for direct contact.[52-54] The highest resolution achieved has been 145 nm through the use of PLL. Improvement of the silver layer could make PLL a viable next generation lithography technique.

2.4 X-ray Nanolithography

The short wavelengths of X-rays give improved diffraction limits compared to optical lithography. Broadband X-rays, typically from a compact synchrotron radiation source, are used to illuminate masks placed in proximity to a resist-coated wafer. The mask (often prepared by EBL) consists of an X-ray absorber, typically gold, on a membrane that is transparent to X-rays, generally silicon carbide or diamond. There are several good reviews focusing specifically on X-ray lithography.[55-57]

X-rays may generate secondary electrons and while the

fine pattern definition is due principally to Auger electrons with very short path lengths, the secondary electrons may sensitize the resist over a larger region than the X-ray exposure. Although this does not affect the pattern pitch resolution, the image exposure contrast may be reduced by factors up to one half. Structures with resolution of ~ 20 nm and less have been published. Deep X-ray lithography uses very short wavelengths of ~ 0.1 nm with modified procedures, to fabricate deeper structures, sometimes three dimensional, with reduced resolution.

Romanato *et al*. produced a 3-dimensional photonic crystal using X-ray lithography.[4] Two gold masks were used; one that created a square array of square holes and another patterned with two triangular arrays of circular holes. The X-rays were directed onto the resist at different angles to generate different patterns. Finally, a 5 nm gold layer is deposited onto the resist to create the 3D photonic crystal.

Metallic 3-dimensional lattices with cubic and Yablonovite structure have been fabricated by X-ray lithography. Yablonovite, also called the 'three cylinder structure', is a distorted rod-connected diamond structure that can be produced by drilling only three holes. The X-ray lithography method is well adapted to fabricate these 3D lattices. The resolution can be controlled to yield lattice parameters of 200 nm.[4]

2.5 Nanoimprint lithography

Nanoimprint lithography (NIL) is a method of fabricating nanometer scale patterns by mechanical deformation of imprint resist followed by subsequent processes. Because NIL is a pattern transfer process; it is not limited by diffraction, scattering effects, or secondary electrons but it relies on other lithography techniques to generate templates. However, it is possible that self-assembled structures could provide templates of periodic patterns at scales of 10 nm and less. Two processes are used for NIL; thermoplastic nanoimprint lithography and step-and-flash nanoimprint lithography.

Thermoplastic nanoimprint lithography (T-NIL) is the more mature nanoimprint lithography. In a standard T-NIL process, a thin polymer layer of imprint resist is spin coated onto a substrate and a mold is brought into contact with the sample and pressed under pressure. When heated above the glass transition temperature of the polymer, the pattern on the mold is pressed into the polymer film. After cooling, the mold is separated from the sample and the pattern remains imprinted on the substrate.

Step and flash imprint lithography (SFIL) uses a UV curable liquid resist and the mold is normally a transparent material like fused silica. After the mold and the substrate are pressed together, the resist is cured with UV light. After mold separation, a pattern transfer process can be used to transfer the pattern onto the material below.

Li *et al*. used microcontact printing as a soft lithographic process to produce a structure on a bis(ω-trimethylsiloxyundecyl)disulfide (TMS) self-assembled monolayer SAM.[58] A stamp made of poly(dimethylsiloxane) (PDMS) was "inked" with a gold nanoparticle solution and brought into contact with the TMS SAM on a gold substrate. Removal of the stamp from the substrate followed by rinsing revealed the pattern. Microcontact printing by Li *et al*. employed ink transfer from an elastomeric stamp to a solid substrate. The ink contained ~4 nm diameter gold spheres. The advantage of this lithographic process is that no diffusion occurs upon transfer, allowing more accurate pattern transfer than normal microcontact printing, which relies on absorbate diffusion from the stamp interior to the surface.

Li *et al*. fabricated optically-functional structures using NIL.[5] A PMMA resist was spin-coated onto a substrate, and a mold was then imprinted into the resist. The compressed PMMA was then removed by anisotropic oxygen etching and a gold layer was evaporated onto the sample before the remaining PMMA was lifted off. The mask produced circular concentric gratings with line widths of about 20 nm. Optical elements can be made with low cost and high throughput.

Similarly, Yu *et al*. used NIL with PMMA resists to create double layer sub-wavelength metal gratings.[59] This was achieved by bypassing the 'lift-off' step listed above. The gold metal gratings are separated by the height of the PMMA layer, allowing different optical properties depending on the amount of the PMMA deposited. NIL has the capability to mold several square centimetres simultaneously but the resolution is lower compared to many other lithographic techniques.

2.6 Scanned probe lithography

There are several different Scanned Probe Lithographic (SPL) techniques, including AFM and STM atom manipulation, and Dip Pen Nanolithography (DPN). Several good reviews of these specific SPL techniques have been published.[60-64]

AFM and STM use a cantilever tip to push atoms around on surfaces to create patterns. DPN is a SPL technique in which a microscopic "pen" is coated with a chemical compound and brought into contact with a substrate to "write" on the substrate with the compound.

AFM has been used to manipulate gold nanorods, fabricated electrochemically, across a silicon substrate.[65] The nanorods were manipulated using the AFM cantilever, which moved the rods along their transverse and longitudinal axis and could also adjust their rotational orientation. This process provides precise control over position and orientation, and is therefore useful as a basis for building more complex nanostructures.

Direct AFM manipulation has been used to create a straight line of 30 nm gold particles. Colloids of 30 nm diameter gold nanoparticles were deposited onto a substrate and the particles were assembled into a straight line using an AFM in contact mode.[14]

Dip-Pen Nanolithography (DPN) was used to fabricate and functionalise Au nanostructures on a semiconductor substrate.[6] An AFM tip was used to deliver molecules to a surface via a solvent meniscus. This direct-write technique offers high-resolution patterning capabilities for a number of

molecular and biomolecular "inks" on a variety of substrates including metals, semiconductors, and monolayer functionalized surfaces. DPN allows control to precisely pattern structures with very accurate positioning. The AFM tip may be used to read, as well as write, nanoscopic features on a surface. Creating nanostructures using DPN is a single step process that does not require the use of resists. Using a conventional AFM, it is possible to achieve ultra-high resolution features with line widths as small as 10-15 nm and with ~ 5 nm spatial resolution.

Mirkin *et al*. fabricated gold-containing nanostructures on a silicon substrate coated with successive layers of silicon oxide (500 nm), titanium (1 nm) and a top layer of gold (8-10 nm).[6, 66-68] Using an AFM tip coated with octadecanethiol [68] or 16-mercaptohexadecanoic acid (MHA) [6,66,67], the thiol was 'written' onto the gold surface. The bound thiol acts as a positive resist and the surrounding areas of the gold/titanium layers were etched using ferricyanide and hydrofluoric acid solutions. The thiol was then photooxidised by irradiation with UV light whereupon it detaches from the surface. The thiol was replaced with an α,ω-dithiol ($HS\text{-}C_6H_{12}\text{-}SH$) or an aminothiol ($HS\text{-}C_2H_4\text{-}NH_2$) compound and the sample immersed in a gold colloid solution whereupon gold nanoparticles adsorbed to the SAM to give the gold/SAM/gold nanoparticle structures. Sub-50 nm arrays of lines and dots were produced using this technique. As well as functionalising the nanostructures with gold nanoparticles, biofunctionalisation was also demonstrated. After the ferricyanide / HF etching steps, any exposed silicon oxide surface was passivated with octadecyltrimethoxysilane and rabbit IgG proteins were then bound to the carboxylic acid groups of the mercaptohexadecanoic acid layer. This procedure therefore generates nanoscale features functionalised with proteins, which may be useful in biosensing applications.

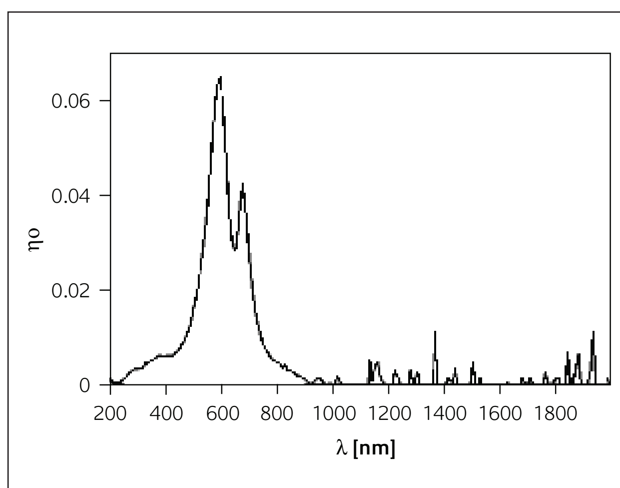

Figure 8

Measured transmittance of the fabricated gold grid. Reprinted from Ref. 8, Jefimovs et al., J. Mod. Opt., ***51****, 1651 (2004) by permission of Taylor & Francis Group. ©2004 Taylor & Francis Ltd (http://www.tandf.co.uk/journals)*

2.7 Island Lithography

Green *et al*. used water vapour to induce the reorganisation of cesium chloride (CsCl) thin films into disordered arrays of hemispherical islands.[9] A thin metal layer (gold or silver) was then deposited onto the structured CsCl film. The CsCl islands, and the thin metal layer attached to them, were removed by immersion in an ultrasonic bath to leave a perforated metallic film. The growth rate of the islands was found to be dominated by the kinetics of dissolution and deposition at the solid/solution boundary.[69] The structured cesium chloride film has also been used as a mask for reactive ion etching.[9] Although this technique does not allow direct writing of specific structures, it is useful for creating patterns that are uniform over a large area.

3 Optical applications of nanoscale gold structures

The optical properties of nanostructured materials often depend upon shape, composition, and the surrounding medium. It is this factor that has motivated much of the interest in using nanolithography to produce precious metal structures. In this section we briefly review some of the applicable nanoscale precious metal structures that have useful optical properties.

3.1 UV-Visible and IR optical absorption filters

Manufacturing filters that block near-infrared radiation but transmit shorter wavelengths is a challenging task that has attracted some interest. Metallic grids fabricated by Jefimovs *et al*. were designed to screen an X-ray detector from incoming heat.[8] The grid structure (Figure 3) is made of 200 x 200 nm square voids separated by 100 nm of metal in each direction. The transmittance of the gold grid is shown in Figure 8. Transmittance of wavelengths longer than 900 nm is low although the transmission observed at visible wavelengths is much lower than theoretical models predict. Interestingly, the square aperture grid structure showed 10% higher transmission compared to the grid with circular apertures.

Similarly, Green *et al*. measured the transmission spectra of perforated thin Ag films prepared using island lithography (see section 2.7. Island Lithography).[9] Figure 9 shows the voids in the film where the hemispheres were removed. The transmission of the perforated films was much higher than the transmission of solid films of similar thickness. Disordered arrays of sub-wavelength diameter cylindrical holes have total transmission efficiencies approaching unity, therefore it was concluded that light can couple efficiently to the surface plasmons.[9]

Johannsmann and Lemke reported an IR resonant filter in the wavelength range of 30-200 μm for use in a space-based telescope.[10] The process and structural properties are very similar to Jefimov's work discussed above. Several different

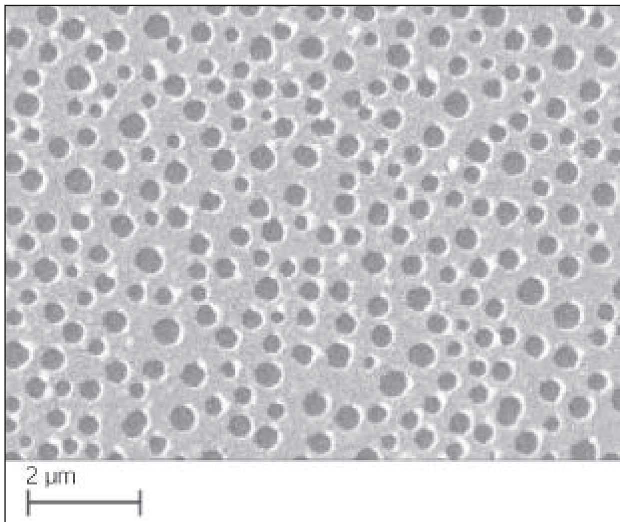

Figure 9
SEM image of perforated metal film (Ag) on a glass substrate. Reprinted from Ref. 9, Green et al., Thin Solid Films, ***467****, 308 (2004) with permission from Elsevier*

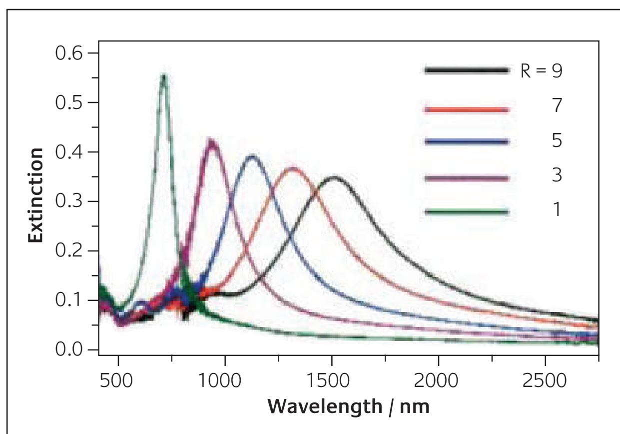

Figure 10
Extinction spectra of gold nanoblocks with different aspect ratios (R) for light polarized parallel to the direction of the rectangular blocks' elongation. Reprinted with permission from Ref. 2, Ueno et al., Opt.Lett., ***30****, 2158 (2005). © 2005 Optical Society of America*

meshes were prepared with variations in the dimensions of the cross shapes and their spacing. These structures allowed transmission of specific broadband wavelengths at ~80% transmission. Changing the size of the crosses and their spacing allowed the structures to be tuned for a specific wavelength and also for the transmittance peak to be broadened or narrowed accordingly.

Ueno *et al*. fabricated gold nanorods with aspect ratios varying from 1 to 9 onto a glass substrate using EBL. The transverse and longitudinal plasmon absorption bands were sensitive to the rods size, aspect ratio, and alignment.[2] For example, rods with an aspect ratio of 9 has a broad absorption band at ~1500 nm whereas rods with an aspect ratio of 1 had a much narrower, intense with a peak at ~ 700 nm. Figure 10 shows the absorption spectra for rods of different aspect ratio.

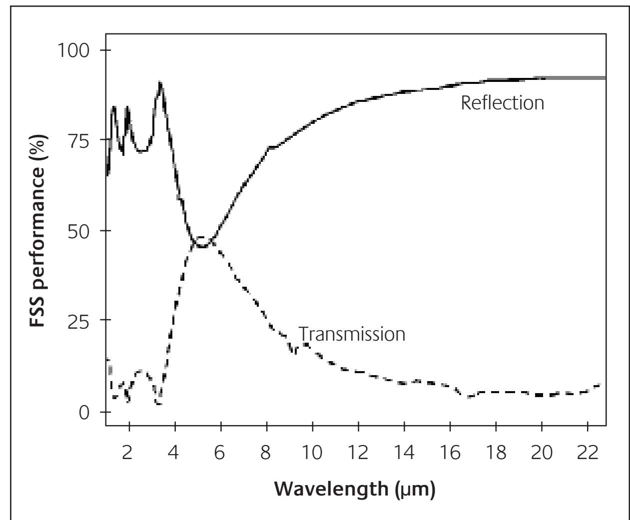

Figure 11
Performance of gold FSS at normal and near normal incidence.[3] Reprinted with permission from Ref. 3, Spector et al., J. Vac. Sci. Technol. B, ***19****, 2757 (2001). © 2001 American Vacuum Society*

A frequency selective surface (FSS) structure was fabricated that could function as an optical filter. Fabrication was achieved using UV lithography with the use of a phase shift mask.[3] The phase shift mask allowed for resolution enhancements to fabricate feature sizes as small as 50 nm. The structure contained circular or hexagonal shaped cylinders within a gold layer. Figure 11 shows the optical properties of the structure. The resonant wavelength, observed at about 5 µm, can be altered by changing the structure and dimensions of the cylinders or the thickness of the gold film. It was suggested that it is possible to increase the transmission at the resonant wavelength above 50% by changing from silicon to a more transparent substrate.[3] This structure is potentially useful in the communications industry as it filters almost all radiation except for that of the resonant band.

Colloidal lithography was used by Hanarp *et al*. to fabricate short range, ordered arrays of nanometre sized gold disks. The dimensions of the gold disks, spacings between the disks and the height of the disks, all combine to vary optical properties of the material. With increasing aspect ratio, a linear increase in plasmon resonance wavelength and an approximately constant peak-width was observed.[13] The sensitivity of the plasmon resonance wavelength to changes in surrounding refractive index is substantially increased for more elongated disks, suggesting that these structures may have potential use in sensors based on the localized surface plasmon resonance change with refractive index.

3.2 Diffraction gratings and photonic crystals

Photonic crystals are periodic materials that allow light to be controlled and manipulated. The utilization of an optical band-gap for optoelectronic applications is believed to require three dimensional photonic crystals that permit full directional control of the light, which holds information.

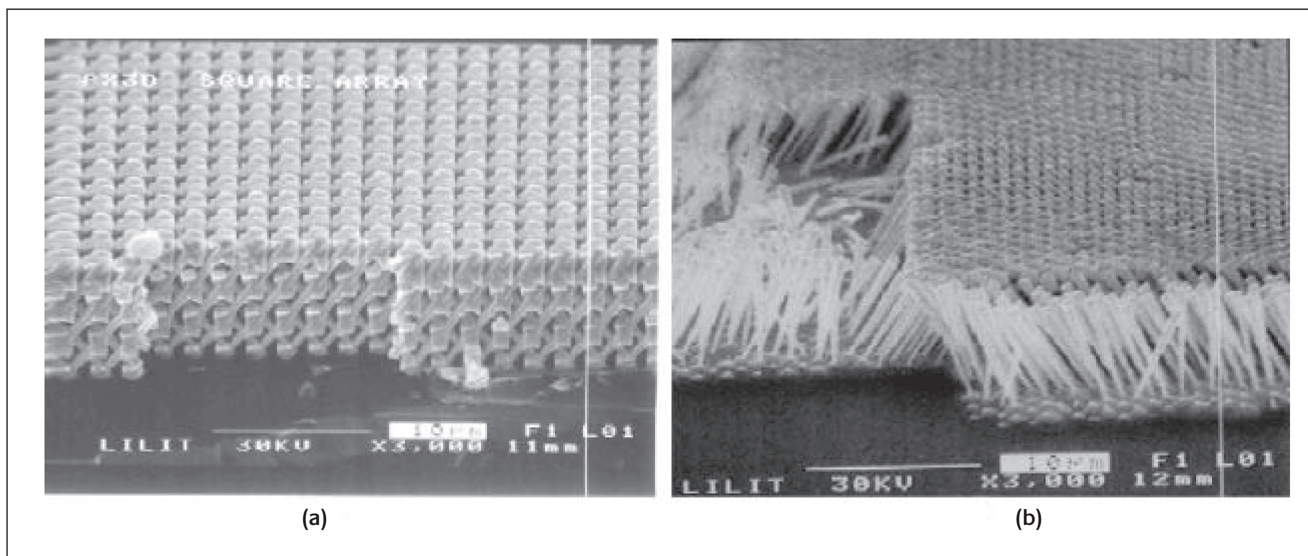

Figure 12

SEM image of a (a) 3D nickel lattice structure obtained by fourfold X-ray exposure of a square pattern array. (b) Yablonovite gold lattice obtained by threefold exposure of a triangular pattern array. Reprinted from Ref. 4, Romanato et al., Microelectron. Eng., ***67-68****, 479 (2003) with permission of Elsevier*

Nanolithography has the potential to create photonic crystals although fabrication may take longer than other methods.

Romanato *et al.* utilised X-ray lithography to fabricate three dimensional photonic crystals using gold and nickel (see 2.4. X-ray Nanolithography).[4] Soft X-ray lithography was used as it provides a high lithographic resolution. A tilted illumination of a symmetric array pattern (through a mask) generates an array of tilted pillars. When another exposure is performed after a rotation of the mask and sample system, a second array of pillars is generated. If the rotation angle is an angle of symmetry, the second pillar array intersects the first one at 3D lattice points. Repetition of this procedure over the entire mask pattern results in the generation of the full three dimensional lattice. For example in the case of square symmetry four exposures in 90° steps generate a cubic lattice. Figure 12 shows two patterns created by this technique. Figure 12(a) shows a SEM image of a cubic nickel lattice. Figure 12(b) shows the Yablonovite gold structure, generated by three 120° step exposure of an equilateral triangle mask array. Preliminary optical characterisation of a cubic metallic lattice showed the presence of resonance features, which are likely to be associated with the excitation of the 3D photonic bands of the metallic sample.[4]

Guo *et al.* recorded the optical spectra of gold diffraction gratings. It was possible to excite a particle plasmon only when the incident light polarization was perpendicular to the grating lines (Transverse Magnetic (TM) polarisation).[44] Hence, the coupling effect between waveguide mode and gold-particle plasmon resonance appears only in TM polarisation. For Transverse Electric (TE) polarisation (parallel to the grating lines) only the waveguide can be excited. These effects are evident from the data shown in Figure 13. Increasing the period of the gold grating structure shifts the lower polarisation branch peak (the longer wavelength peak in Figure 13(a)) towards a longer wavelength due to the larger

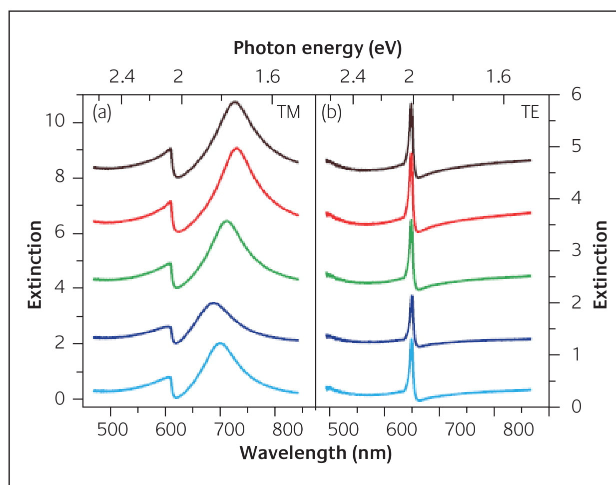

Figure 13

Extinction of a gold grating, taken at different positions on the sample (a) TM polarization, (b) TE polarization. Reprinted from Ref. 44, Guo et al. Appl. Phys. B, **81***, 271 (2005) with kind permission of Springer Science and Business Media*

wire width. The extinction characteristics investigated by Guo *et al.* indicate that strong coupling exists between waveguide mode and particle plasmon appears when the waveguide is tuned into the plasmon resonance.[44]

Lamprecht *et al.* investigated the influence of grating effects on plasmon excitations in gold nanoparticles produced by EBL.[20] Results show an increase in plasmon damping in the transition region from evanescent to radiative fields (500 nm – 600 nm) of the first grating order on the substrate side. A strong red-shift of approximately 50 nm in the plasmon resonance wavelength was also observed in this transition region. It was found that the shift and broadening of the plasmon resonance are fundamentally determined by the periodicity of a square array. The dipolar fields of neighbouring

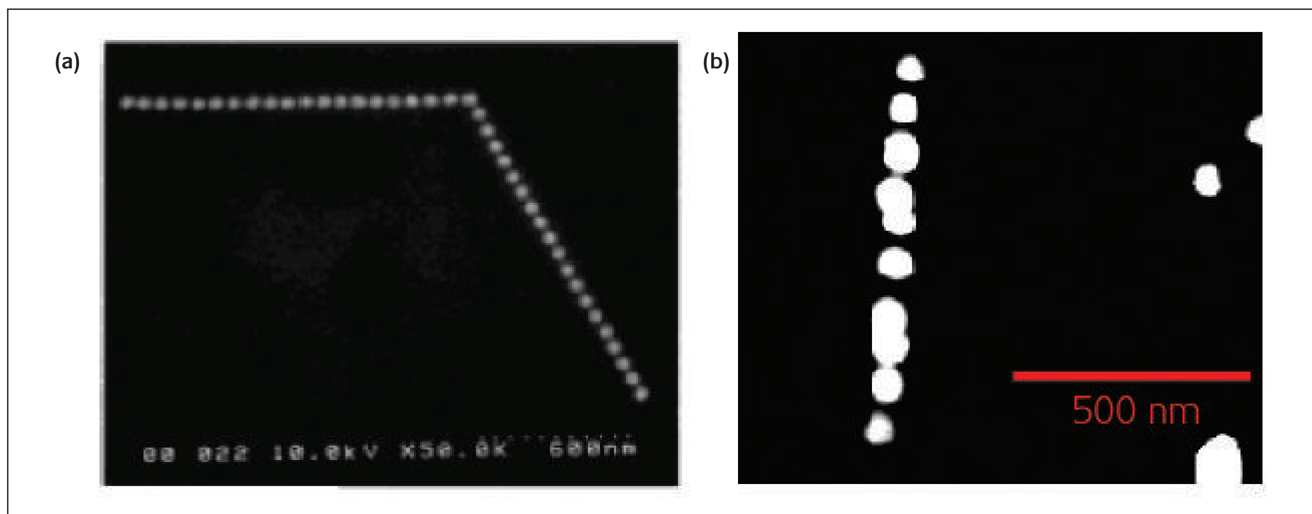

Figure 14

(a) SEM image of 60° corner in a plasmon waveguide fabricated by EBL. (b) Straight plasmon waveguide assembled using contact mode AFM and imaged using non-contact AFM.[14] Reprinted with permission from Ref. 14, Maier et al., Adv. Mater., **13***, 1501 (2001)*

particles are superimposed with their respective phase shifts, which depend on the distance between the particles. Thus the geometrical arrangement of resonant metal nanoparticles in their respective far field regions significantly affects the individual particle plasmon and thus the plasmon near-field characteristics.

For single layer sub-wavelength metal grating polarisers with fixed periods, polarisation anisotropy increases as the wavelength increases. Yu *et al.* fabricated a dual layer grating which shows an extinction ratio maximum in the visible region, indicating resonance occurs between the two metal grating layers. Resonance between the layers helps to enhance the polarization selectivity for wavelengths close to 630 nm. Due to resonance effects, high polarization extinction ratios at certain wavelengths can be more easily achieved with a double-layer metal grating structure.[59]

3.3 Waveguides

Planar waveguides are useful optical devices that can be used to guide electromagnetic radiation enabling the integration of nano-photonic devices in optical circuitry. By utilising the plasmon resonance of gold nanoparticles, plasmonic waveguides may be fabricated that guide electromagnetic radiation in the visible and near-infrared region of the spectrum. Excitation at or near the plasmon resonance allows radiation to couple to nearby particles. In plasmonic waveguides, a row of appropriately spaced nanoparticles can transfer energy from one particle to another, thus propagating a wave.[14]

Maier *et al.* used EBL and AFM manipulation to construct functional plasmonic waveguides.[14] Figure 14(a) shows a 60° corner structure fabricated using EBL on ITO-doped glass. The gold particles are 50 nm in diameter and are separated by 75 nm (centre to centre). Figure 14(b) shows a linear plasmon waveguide using 30 nm colloidal gold nanoparticles. A line was constructed by aligning randomly deposited gold nanoparticles using an AFM tip. These plasmonic waveguides show potential for use in nanoscale integrated optics especially as light can be efficiently guided around corners, which is a limitation of conventional planar waveguides due to radiation leakage at sharp bends.

4 Conclusions

Lithography techniques play an important role in the fabrication of functional devices based on nanoscale structures of the precious metals. Once a pattern or design has been identified by simulation or calculation, it can be fabricated using one or more of the technologies that we have described here. Each of the lithography systems is based on fundamentally different physical properties, implying that each technique will exhibit unique properties. Gold is a good choice of metal for use in nanoscale optical devices as it is relatively inert, easily deposited, and has surface plasmons that can be tuned by dimensional control from the mid-visible to the near-infrared.

About the authors

All the authors are at the University of Technology Sydney (UTS), in Australia.

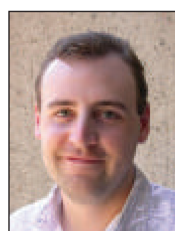

Nick Stokes is studying for his PhD in the UTS Institute for Nanoscale Technology. His project is co-funded by mining company Anglogold Ashanti Limited and the Australian Research Council and is focussed on developing gold-based, spectrally selective coatings for glass.

Dr Andrew McDonagh is a Senior Lecturer at in the Department of Chemistry, Materials and Forensic Sciences at UTS and is also a member of its Institute for Nanoscale Technology. Andrew specializes in inorganic and physical chemistry.

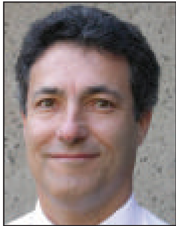

Professor Michael Cortie is Director of the UTS Institute for Nanoscale Technology. His interests include materials science and engineering and the optical properties of nanoscale structures.

Acknowledgement

This work has been supported by the Australian Research Council (LP0560475) and by resources and mining company AngloGold Ashanti.

References

1 M. Cortie, *Gold Bull*., 2004, **37**, 12
2 K. Ueno, V. Mizeikis, *et al*., *Opt. Lett*., 2005, **30**, 2158
3 S. Spector, D. Astolfi, *et al*., *J. Vac. Sci. Technol., B*, 2001, **19**, 2757
4 F. Romanato, L. Businaro, *et al*., *Microelectron. Eng*., 2003, **67-68**, 479
5 M. Li, J. Wang, *et al*., *Appl. Phys. Lett*., 2000, **76**, 673
6 H. Zhang, K. Lee, *et al*., *Nanotechnology*, 2003, **14**, 1113
7 M. Mützel, S. Tandler, *et al*., *Phys. Rev. Lett*., 2002, **88**, 083601
8 K. Jefimovs, T. Vallius, *et al*., *J. Mod. Opt*., 2004, **51**, 1651
9 M. Green and F. Yi, *Thin Solid Films*, 2004, **467**, 308
10 D. Johannsmann and D. Lemke, *Infrared Phys*., 1986, **26**, 215
11 A. Perentes, I. Utke, *et al*., *Nanotechnology*, 2005, **16**, 273
12 M. Fukushima, H. Yanagi, *et al*., *Thin Solid Films*, 2003, **438-439**, 39
13 P. Hanarp, M. Kall, *et al*., *J. Phys. Chem. B*, 2003, **107**, 5768
14 S. Maier, M. Brongersma, *et al*., *Adv. Mater*., 2001, **13**, 1501
15 X. Ngo and C. Rosilio, *Nucl. Instrum. Meth. Phys. Res. B*, 1997, **131**, 22
16 D. Ferry, M. Khoury, *et al*., *Semicond. Sci. Technol*., 1996, **11**, 1552
17 Y. Chen and A. Pepin, *Electrophoresis*, 2001, **22**, 187
18 J. Wei and K. Wong, *Int. J. Nanosci*., 2005, **4**, 575
19 W. Gotschy, K. Vonmetz, *et al*., *Appl. Phys. B*, 1996, **63**, 381
20 B. Lamprecht, G. Schider, *et al*., *Phys. Rev. Lett*., 2000, **84**, 4721
21 M. Klein, C. Enkrich, *et al*., *Science*, 2006, **313**, 502
22 C. Enkrich, M. Wegener, *et al*., *Phys. Rev. Lett*., 2005, **95**, 203901
23 S. Linden, C. Enkrich, *et al*., *Science*, 2004, **306**, 1351
24 J. Pendry and D. Smith, *Phys. Today*, 2004, **57**, 37
25 D. Smith, J. Pendry, *et al*., *Science*, 2004, **305**, 788
26 A. Grigorenko, A. Geim, *et al*., *Nature*, 2005, **438**, 335
27 F. Garwe, C. Rockstuhl, *et al*., *Appl. Phys. B*, 2006, **84**, 139
28 S. Griffith, M. Mondol, *et al*., *J. Vac. Sci. Technol*., B, 2002, **20**, 2768
29 F. Watt, A. Bettiol, *et al*., *Int. J. Nanosci*., 2004, **4**, 269
30 S. Reyntjens and R. Puers, *J. Micromech. Microeng*., 2001, **11**, 287
31 S. Matsui, T. Kaito, *et al*., *J. Vac. Sci. Technol., B*, 2000, **18**, 3181
32 T. Morita, K. Watanabe, *et al*., *Jpn. J. Appl. Phys*., Part 1, 2003, **42**, 3874
33 J. Fujita, M. Ishida, *et al*., *Nucl. Instrum. Meth. Phys. Res. B*, 2003, **206**, 472
34 R.J. Young, J.R.A. Cleaver, *et al*., *J. Vac. Sci. Technol., B*, 1993, **11**, 234
35 I. Chyr and A.J. Steckl, *J. Vac. Sci. Technol., B*, 2001, **19**, 2547
36 Y. Liu, D.M. Longo, *et al*., *Appl. Phys. Lett*., 2003, **82**, 346
37 J.A. van Kan, A.A. Bettiol, *et al*., *Appl. Phys. Lett*., 2003, **83**, 1629
38 F. Lison, H. Adams, *et al*., *Appl. Phys. B*, 1997, **65**, 419
39 R. Seisyan, *Tech. Phys*., 2004, **50**, 535
40 B. Fay, *Microelectron. Eng*., 2002, **61-62**, 11
41 M. Rothschild, *Mater. Today*, 2005, **8**, 18
42 M. Alkaisi, R. Blaikie, *et al*., *Adv. Mater*., 2001, **13**, 877
43 T. Brunner, *J. Vac. Sci. Technol., B*, 2003, **21**, 2632
44 H. Guo, D. Nau, *et al*., *Appl. Phys. B*, 2005, **81**, 271
45 Y. Nakata, T. Okada, *et al*., *Appl. Phys. A*, 2004, **79**, 1481
46 H. Solak, *J. Phys. D: Appl. Phys*., 2006, **39**, R171
47 R. Gronheid, H. Solak, *et al*., *Microelectron. Eng*., 2006, **83**, 1103
48 S. Sun, P. Mendes, *et al*., *Nano Lett*., 2006, **6**, 345
49 D. Chao, A. Patel, *et al*., *J. Vac. Sci. Technol., B*, 2005, **23**, 2657
50 W. Jung, F. Castaño, *et al*., *J. Vac. Sci. Technol., B*, 2004, **22**, 3335
51 H. Smith, R. Menon, *et al*., *Microelectron. Eng*., 2006, **83**, 956
52 D. Melville, R. Blaikie, *et al*., *Curr. Appl. Phys*., 2006, **6**, 415
53 R. Blaikie, D. Melville, *et al*., *Microelectron. Eng*., 2006, **83**, 723
54 D. Melville, R. Blaikie, *et al*., *Appl. Phys. Lett*., 2004, **84**, 4403
55 H. Smith, M. Schattenburg, *et al*., *Microelectron. Eng*., 1996, **32**, 143
56 F. Cerrina, *J. Phys. D: Appl. Phys*., 2000, **33**, R103
57 H. Smith, *J. Vac. Sci. Technol., B*, 1995, **13**, 2323
58 X. Li, V. Paraschiv, *et al*., *J. Am. Chem. Soc*., 2003, **125**, 4279
59 Z. Yu, P. Deshpande, *et al*., *Appl. Phys. Lett*., 2000, *77*, 927
60 K. Wilder, H. Soh, *et al*., *J. Vac. Sci. Technol., B*, 1997, **15**, 1811
61 R. Garcia, R. Martinez, *et al*., *Chem. Soc. Rev*., 2006, **35**, 29
62 K. Wilder, C. Quate, *et al*., *J. Vac. Sci. Technol., B*, 1998, **16**, 3864
63 I. Sung and D. Kim, *Appl. Surf. Sci*., 2005, **239**, 209
64 Q. Tang, A. Shi, *et al*., *J. Nanosci. Nanotechnol*., 2004, **4**, 948
65 S. Hsieh, S. Meltzer, *et al*., *J. Phys. Chem. B*, 2002, **106**, 231
66 H. Zhang, S. Chung, *et al*., *Nano Lett*., 2003, **3**, 43
67 H. Zhang, Z. Li, *et al*., *Adv. Mater*., 2002, **14**, 1472
68 R. Piner, J. Zhu, *et al*., *Science*, 1999, **283**, 661
69 M. Green and S. Tsuchiya, *J. Vac. Sci. Technol., B*, 1999, **17**, 2074